Characteristics and impacts of La Niña diversity on Pacific teleconnections

Mandy B. Freund[1,2*], Hanna Heidemann[1,2,3], Aditya Sengupta[1,2], Ruby Lieber[1,4], Navid C. Constantinou[1,2]

[1]School of Geography, Earth and Atmospheric Sciences, University of Melbourne, Parkville, 3010, VIC, Australia.
[2]Australian Research Council Centre of Excellence for the Weather of the 21st Century, University of Melbourne, Parkville, 3010,VIC, Australia.
[3]Centre for Applied Climate Sciences, University of Southern Queensland, Toowoomba, 4350, QLD, Australia.
[4]School of Geographical Sciences, University of Bristol, Bristol, BS8 1QU, United Kingdom.

*Corresponding author(s). E-mail(s): mandy.freund@unimelb.edu.au;
Contributing authors: hanna.heidemann@unimelb.edu.au; aditya.sengupta@student.unimelb.edu.au; ruby.lieber@bristol.ac.uk; navid.constantinou@unimelb.edu.au;

Abstract

Motivated by the 2020-2023 triple-dip La Niña event, with central Pacific (CP) events in 2020 and 2022 bracketing an eastern Pacific (EP) event in 2021, we examine how La Niña diversity impacts Pacific teleconnections. Although CP/EP El Niño diversity and its atmospheric impacts are well studied, comparable distinctions among La Niña events remain less developed. Using observations, reanalysis, and ocean model output, we characterise the seasonal evolution of CP and EP La Niña events in oceanic structure, atmospheric circulation, rainfall, and biological productivity. CP La Niña events exhibit broader meridional and stronger equatorial Pacific cooling, enhanced western Pacific subsurface warming, and a stronger atmospheric zonal circulation, producing intensified rainfall over the Maritime Continent and northern Australia. EP La Niña events show confined eastern Pacific cooling that persists into austral autumn, alongside a weaker but longer-lived mid-latitude atmospheric response and enhanced South America rainfall. Our results highlight how distinguishing La Niña diversity could

help resolve currently unconstrained impacts, including those associated with prolonged La Niña events under future warming.

Keywords: ENSO diversity, La Niña, Rainfall, Teleconnections, Tropical Pacific

Introduction

The El Niño Southern Oscillation (ENSO) is the primary driver of year-to-year climate variability in the Earth system, altering atmospheric circulation patterns and triggering widespread ecological and societal impacts [1–3]. While ENSO's warm phase (El Niño) has received considerable attention [4–8] due to its stronger intensity and immediate socio-economic impacts [1, 8], its cool phase, La Niña, has been historically understudied. However, in recent years, La Niña events have gained significant traction as they could become a more frequently occurring feature of our global climate under anthropogenic warming [9–11]. La Niña events are characterised by cooler-than-normal sea surface temperatures (SST) in the central to eastern equatorial Pacific Ocean, and influence atmospheric temperature and precipitation patterns worldwide [12]. The three consecutive La Niña events between 2020 and 2023 (also referred to as a 'triple-dip La Niña'), exemplified the far-reaching consequences of these cool phase events, contributing, among other things, to devastating floods in Australia [13], an extremely active Atlantic hurricane season [14], and disruptions to precipitation patterns across multiple continents [15, 16]. These multi-year La Niña conditions not only drive persistent rainfall deficits and temperature anomalies within individual event years, but add cumulative risk of extreme weather [17], including drought and wildfires in the southwestern United States [18, 19] and flooding over Southeast Asia [20].

Although the different manifestation of the SST patterns associated with La Niña events have global impacts, our understanding of its diversity remains far from complete, especially compared to its El Niño counterpart. While central Pacific (CP) and eastern Pacific (EP) El Niño events exhibit distinct spatial patterns [21], La Niña events are more subtle in their SST pattern differences [22], making them more difficult to distinguish. However, La Niña events may display a less subtle diversity in their teleconnections [23]. As shown in previous studies, some La Niña events are more intense, persistent, or coupled with distinct atmospheric patterns that lead to regional variations in their impacts on temperature, precipitation, and extreme weather events [24, 25].

Besides the recent triple-dip La Niña events cumulating in prolonged extreme climate disruptions, this sequence of events uniquely featured alternating types of La Niña events [26]. Generally, most of La Niña-related SST variability occurs in the Central Pacific. While this was the case for the first and third of the recent sequence of events, the second La Niña over 2021/2022 featured more pronounced cooling in the eastern side of the Pacific [27]; see also Fig. 1. These differences in SST cooling patterns between individual La Niña years could also explain the different large-scale impacts associated with, e.g., the first and second La Niña in this multi-year event. In turn, spatial differences in the peak location of SST cooling could drive substantial

atmospheric teleconnection differences that modulate precipitation and temperature anomalies across disparate global regions [28]. The characteristics and impacts of different types of La Niña events is the central theme of this paper.

Motivated by the above discussion, in this paper we strive to address *(i)* the potential advantages of distinguishing between CP and EP La Niña events and, *(ii)* to quantify their commonalities and differences in associated oceanic and atmospheric patterns. We show that as our understanding of ENSO deepens, distinct "flavours" of La Niñas merits recognition, particularly concerning their influences on hydroclimatic impacts around the Pacific. We demonstrate that by disentangling potential analogues within the La Niña events, we can refine impact-based forecasting, risk assessments, and tailored adaptation strategies for regions differentially affected by the varying manifestations of these events.

Recent triple-dip La Niña event

The SST cooling patterns during the peak phase (December to February) of the three recent consecutive La Niña events from 2020-2023 are highlighted in Figure 1. During the 2020/21 La Niña, the most intense cooling was located predominantly in the central Pacific (Fig. 1a); for the second 2021/22 La Niña the most intense cooling occurred in the eastern Pacific (Fig. 1b) and during the 2022/23 La Niña the strongest cooling was again present in the central Pacific (Fig. 1c). Many aspects around this triple-dip La Niña events are unusual. For example, multi-year La Niña events are often thought to be preceded by El Niño conditions [29] but, interestingly, the recent consecutive La Niña events did not follow a strong El Niño event [30, 31] as suggested by heat content discharge mechanism [32]. Instead, research suggests that it is related to a weak precursor El Niño event in 2019 that peaked in the central Pacific [10]. Regardless of what factors initiate the occurrence of multi-year La Niña events, it is the first time that alternating types of La Niña events were observed in consecutive years [26, 27].

Given that the maximum SST cooling patterns for the two types of La Niña events occurred more than 10,000 kilometres apart [33], it is expected that distinct precipitation anomaly pattern differences are observed as well. Focussing on land areas, the more 'traditional' CP La Niña events in 2020/21 and 2022/23 (Fig. 1a,c) exhibited the following commonalities in precipitation anomaly patterns: Both years showed drier than usual conditions in parts of subtropical and Tibetan plateau regions and wetter conditions in cooler parts of Asia. The global pattern correlation of precipitation anomalies over land between these two CP La Niña events is 0.38, indicating some regional similarities. However, correlating precipitation anomalies of 2021/22 with 2022/23 or 2020/21 results in substantially lower pattern correlations ($r < 0.1$). Among the two CP La Niña years, most similarities in rainfall impact appear to occur on the western side of the Pacific (west of 180°E). Interestingly, the EP La Niña in 2021/22 and CP La Niña in 2022/23 (Fig. 1b,c) show closer similarities on the eastern side of the Pacific, including over North and South America.

Overall, the recent multi-year La Niña episode, with its differences in Pacific SST cooling signatures and contrasting large-scale land precipitation anomalies, raises fundamental questions about the inherent variability of La Niña events. To what extent are the observed differences in SST and rainfall deviations between EP and CP events

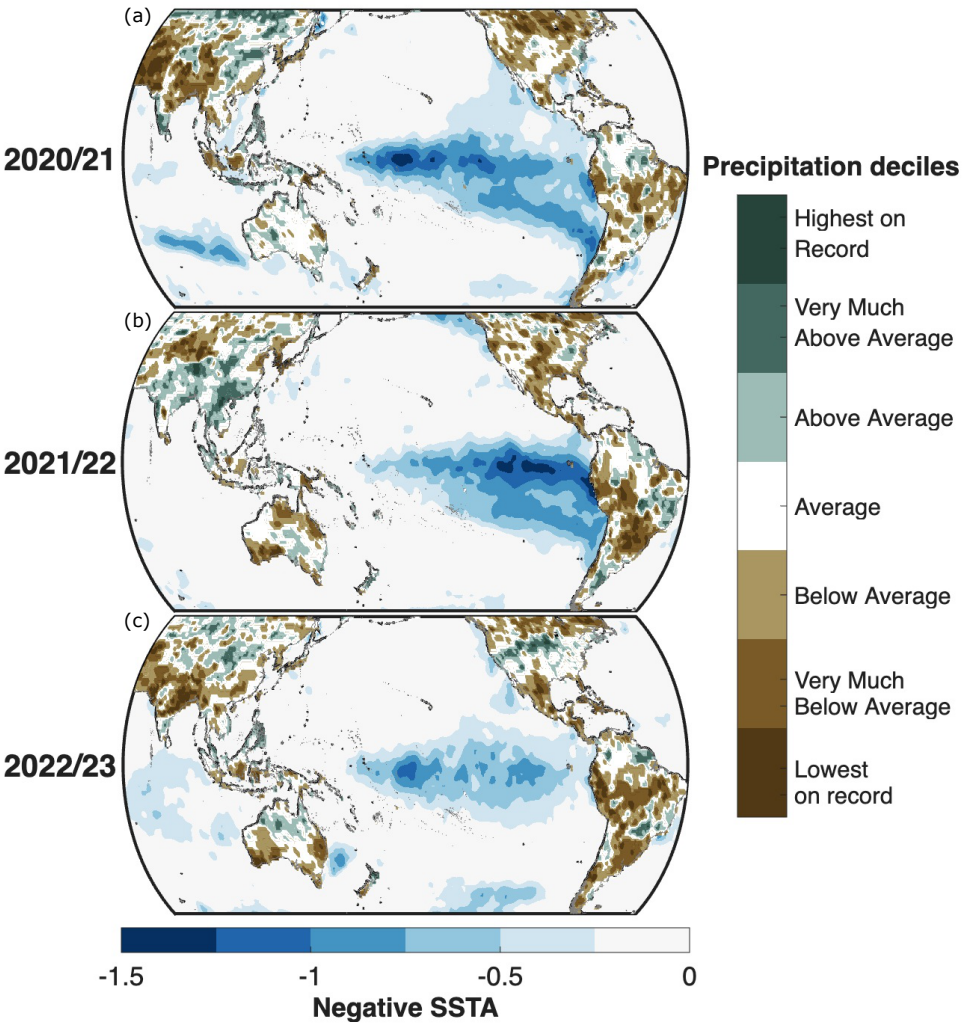

Fig. 1 Sea-surface temperature anomalies (SSTA) (only negative anomalies are shown) and precipitation deciles over land during months DJF (December to February) for the triple-dip La Niña events: (a) 2020/21, (b) 2021/22, and (c) 2022/23. Common baseline period 1920-2025 was used for anomalies.

statistically robust? Do different types of La Niña events exhibit commonalities in their atmospheric and oceanic responses despite the diverse impacts they bring about? In this paper, we elucidate the similarities of past observed La Niña events by focusing on observation and reanalysis data reaching back to the beginning of the 20th century (see Methods section).

Results and Discussion

Distinction of La Niña types

We first examine the temporal signatures of CP and EP La Niña events during 1900 to 2023 using multiple observational datasets. CP La Niña events (sample size $n = 25$), the predominant type, exhibit a wide range of equatorial zonal SST anomalies between events and across all seasons. This is consistent across all three analysed SST datasets: HadISST, ERSST, and COBE (Fig. 2a,d,g). (For more details on datasets see Data section.) In contrast, the magnitude of SST anomalies during the included EP La Niña events ($n = 5$) is more similar across events and throughout the equatorial Pacific. The strongest negative SST anomalies occur in the eastern equatorial Pacific (Fig. 2b,e,h). Both event types show peak cooling during the developing (SON) and mature (DJF) phases, with CP events exhibiting much stronger negative SST anomalies around 180°E compared to EP events.

The contrast between CP and EP La Niña events is most evident in their difference plots (Fig. 2c,f,i). CP events reveal much stronger negative anomalies around 180°E during their developing and mature phases (SON and DJF) compared to EP events, while event type differences in the western Pacific are minimal. EP events show stronger negative SST anomalies in the eastern Pacific during their peak (DJF) and decaying (MAM+) phases, resulting in positive difference anomalies. Notably, CP events demonstrate a quicker recovery to neutral conditions in the eastern Pacific during the decaying phase compared to EP events. The mean equatorial SST anomalies during both types of La Niña events is consistent across the three observational SST products, indicating that the result is robust.

Spatial differences between EP and CP La Niña SST pattern

Figure 3 shows composite large-scale SST anomalies associated with CP and EP Niña events during 1900 to 2023. This figure highlights the seasonal evolution of SST anomalies in the Pacific Ocean in both zonal and meridional directions during both event types, from the development stages (Fig. 3a,b) to its decay (Fig. 3e,f).

During CP La Niña events, the mean SST anomalies show a broader spatial extent in both zonal and meridional directions, as well as more strongly negative significant SST anomalies. Negative SST anomalies stretch well into the Northern and Southern Hemisphere (exceeding 20° North and South), forming a broad, wedge-shaped pattern that is observed from the developing through to the decaying phases (SON through to MAM+1). The strongest negative SST anomalies occur in the developing and mature phase (SON and DJF; Fig. 3a,c). In addition, negative outgoing longwave radiation (OLR) anomalies are observed over the approximate region of the South Pacific Convergence Zone, Maritime Continent and northern Australia that continue through the decaying phase, while OLR anomalies are positive over the central Pacific. Significantly positive SST anomalies are flanking the region of cool SST anomalies to the north and south during all seasons (Fig. 3a,c,e), and in the western Pacific in the developing stage of the event. During this part of the year, they are particularly strong in the Coral Sea, stretching eastwards (Fig. 3a).

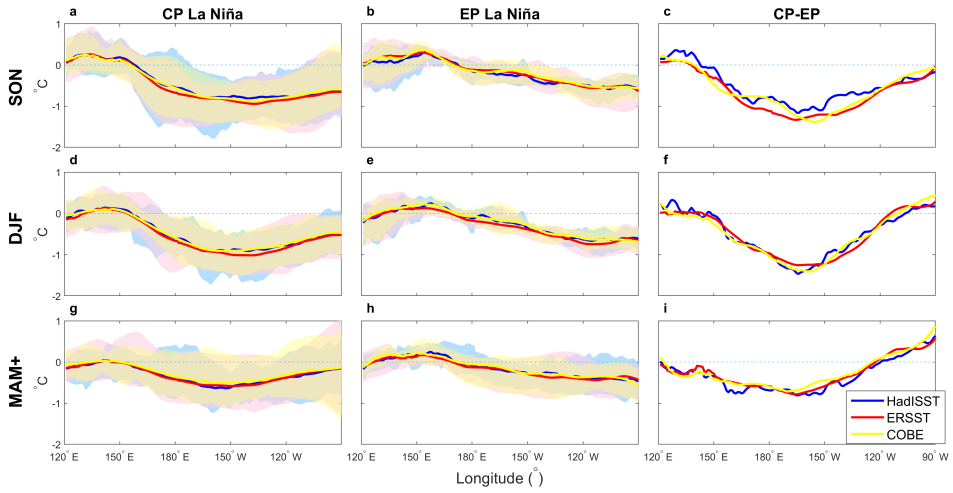

Fig. 2 Zonal sea-surface temperature anomalies during CP and EP La Niña events Composites of SST anomalies during CP and EP La Niña events between 1900 and 2023, averaged over the equatorial Pacific (10°N-10°S) from three different observational datasets: HadISST, ERSST, COBE. Shown are the seasonal averages for months SON (panels a-c), DJF (panels d-f), and MAM+1 (panels g-i). Solid curves indicate mean of the composites; background shading indicates the max-min range of observed SST anomalies for each dataset and event type. The differences between CP and EP La Niña events are shown in the right-most column; panels c, f, i. Anomalies are calculated relative to the 1981–2010 climatology.

In contrast, during EP La Niña events, the composite negative SST anomalies are weaker and occur in the tropical regions only within approximately 20° North and South. The region of significantly negative SST anomalies is much smaller compared to the CP event composite and mostly confined to the eastern Pacific. Furthermore, SST anomalies are only significant in the developing through to the decaying phases (Fig. 3b,d), highlighting the shorter duration of EP events. Positive SST anomalies during EP events are only significant in the north Pacific during the developing and decaying phase (Fig. 3b,f). Interestingly, parts of the western Pacific show significantly negative SST anomalies around the western Maritime Continent and are strongest in the Western North Pacific during the peak and decaying part of the event (Fig. 3d,f).

Subsurface ocean differences between EP and CP La Niña

The vertical ocean temperature anomaly structure during La Niña events also reveals substantial differences between the western and eastern Pacific (Fig. 4). In the western Pacific west of approximately 150-160°W, anomalously warm waters typically extend deep into the subsurface ocean. Conversely, the thermocline shoals toward the east, bringing cooler anomalies closer to the surface. This eastward tilt enhances the cold tongue in the eastern Pacific and reinforces the west–east gradient in subsurface temperatures, characteristic of La Niña events [35]. Both CP and EP La Niña events exhibit cooler-than-normal surface and near-subsurface conditions. However,

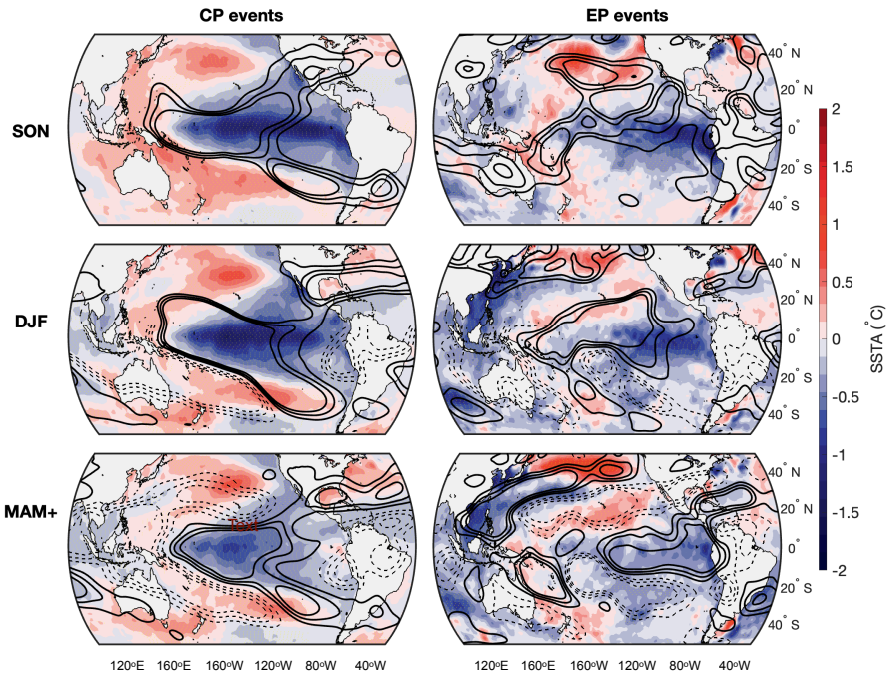

Fig. 3 Composites associated with CP and EP La Niña events of sea-surface temperature anomalies using HadISST (1900-2023). Stippling indicates significance ($p < 0.05$) at the 95th percentile. Solid black curves depict positive OLR anomalies (1900-2015) as computed from Ref. [34]; dashed curves indicates negative OLR anomalies. OLR is shown here as a proxy of cloud coverage.

CP La Niña events develop anomalous warming at around 150 metres below the surface, intensifying from the developing phase through to the decay phase. EP La Niña events also show warm subsurface anomalies in the western tropical Pacific, although these are generally weaker than in CP events (Fig. 4b,e,h). Both CP and EP events exhibit subsurface cooling, but the spatial pattern differs: CP events tend to produce stronger warm anomalies in the western basin together with more prominent subsurface cooling in the central Pacific and relatively weaker cooling near the eastern coastal margins; by contrast, EP events are associated with stronger surface cooling and pronounced negative subsurface anomalies along the eastern Pacific continental margin while often showing relatively warmer subsurface conditions in the central Pacific (Fig. 4c,f,i). These contrasts also affect the thermocline slope (approximated by the 20°C isotherm, indicated by cyan and pink contours in Fig. 4): CP events are associated with a slightly steeper thermocline in the western Pacific, whereas EP events show deeper/eastern cooling that sharpens the zonal gradient. The cooling along the eastern margin during EP events can persist into the decaying phase due to continued upwelling (Fig. 4i). Overall, CP La Niña events produce stronger basin-scale subsurface temperature anomalies during the peak season, but the central versus coastal eastern patterns emphasise the need to distinguish CP and EP event structures.

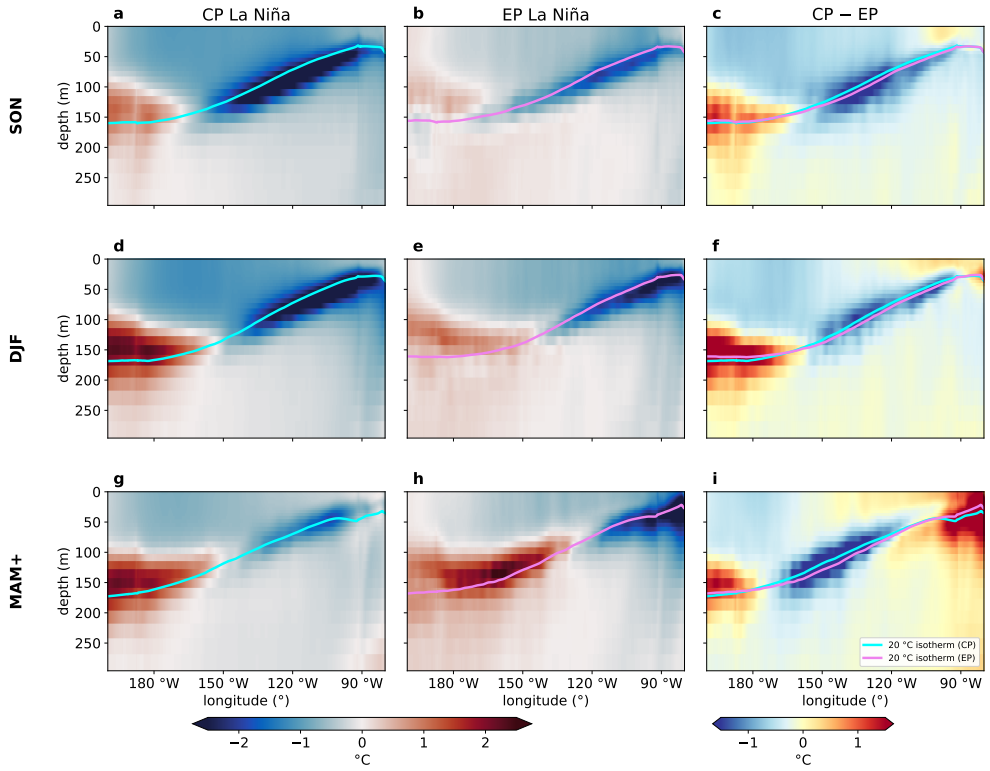

Fig. 4 Composite ocean temperature anomalies in the tropical Pacific (5 °S–5 °N and 140 °E–80 °W) for CP (a, d, and g) and EP (b, e, and h) La Niña, acquired from the ACCESS-OM2-01 ocean–sea ice model. Each row corresponds to different seasons SON, DJF and MAM+; the rightmost column shows the differences of the CP and EP composites. Anomalies are computed using a 1958-2023 climatology and detrending has been applied. The cyan and purple contours mark the 20 °C isotherm for the CP and EP composites, respectively.

Atmospheric differences of EP and CP La Niña

In addition to their contrasting oceanic signatures, EP and CP La Niña events exhibit markedly different atmospheric responses, particularly in the position and intensity of tropical convection, the Pacific Walker circulation, and associated teleconnections. Traditionally, La Niña events are characterised by anomalies in mean sea-level pressure (MSLP) that indicate a strengthening of the Pacific Walker circulation [36]: Lower pressure over the western Pacific and higher pressure over the eastern Pacific create an enhanced east–west pressure gradient along the equator, leading to stronger-than-usual easterly trade winds [12]. Alongside these surface-pressure anomalies, La Niña events exhibit enhanced vertical velocities in the tropical atmosphere, with anomalous ascent over the western Pacific and compensating subsidence over the central to eastern Pacific [37]. However, the zonal atmospheric circulation associated with La Niña differs between its EP and CP types.

During the developing stage (SON), both EP and CP La Niña events already show contrasting patterns in vertical motion around the equator and surface-pressure anomalies (Fig. 5a,b). For CP La Niña events, anomalous sinking motion emerges over the entire equatorial eastern to central Pacific associated with anomalously high MSLP, while rising motion intensifies over the western equatorial Pacific in line with a large-scale decrease in MSLP (Fig. 5a). For EP La Niña, both surface pressure and vertical velocity anomalies around the equator are much less pronounced (Fig. 5b). Significant pressure anomalies are weaker and more localised. In particular, they are restricted to the eastern continental margins of the tropical Pacific and approximately symmetric around the equator. Interestingly, the maximum low-pressure anomalies in the western Pacific are displaced towards higher latitudes compared to those associated with CP events. These anomalies primarily affect the eastern half of Australia, stretching eastwards into the Coral Sea and beyond. In the Northern Hemisphere, lower MSLP is found in the western north Pacific. This pattern is presumably associated with a weakening of the descending branches of the local Hadley cell over these areas [38]. Anomalously high pressure in the eastern Pacific by contrast follows the cooler SST anomaly pattern closely; the anomalies are however very weak. Overall, during the developing phase, the vertical wind velocity anomalies around the equator during EP La Niña are weaker and indicate a less intense strengthening of the Pacific Walker circulation compared to CP La Niña composites (Fig. 5,b).

By the mature phase (DJF), pressure anomalies and vertical motions intensify during both types of La Niña events (Fig. 5,c,d). The CP La Niña composites show a major sinking branch around the western side of the Niño3.4 region (around 180°E) and beyond, accompanied by anomalous ascent over the Maritime Continent as well as on the other side of the Pacific basin, over far continental South America (Fig. 5,c). In contrast, EP La Niña exhibit strong descent further eastward around 150°W and is almost exclusively restricted to the Niño3.4 region. The anomalous ascent in the western Pacific is negligible (Fig. 5,d). During EP La Niña, significant low MSLP anomalies are located in the North Pacific around 20°–30°N. This trough-like feature could indicate an expansion of the Hadley cell during boreal winter, as shown by Guo and Li [38]. This pattern has previously been shown to arise as a result of the subsidence over the eastern to central Pacific, altering the subtropical ridge structure and allowing anomalously low surface pressure to develop further south of the typical location of the Aleutian Low [39]. A deep Aleutian Low during the peak La Niña phase reflects an intensified mid-latitude response to EP La Niña forcing. This may be linked to a negative Pacific North America pattern, which typically brings colder, wetter conditions to the northwestern Pacific and drier, warmer conditions to the southern United States [40].

Associated with the decaying stage of the event (MAM+), vertical motion along the equator weakens in both EP and CP La Niña composites. However, this weakening is stronger during CP La Niña events compared to EP La Niña events (compare Figs. 5e and 5f). A notable contrast emerges: the atmospheric response during CP La Niña events diminishes rapidly after its peak, whereas EP La Niña events maintain a pronounced dynamical signal. During EP La Niña, the anomalous low-pressure region over the North Pacific persists (however substantially weaker compared to the previous

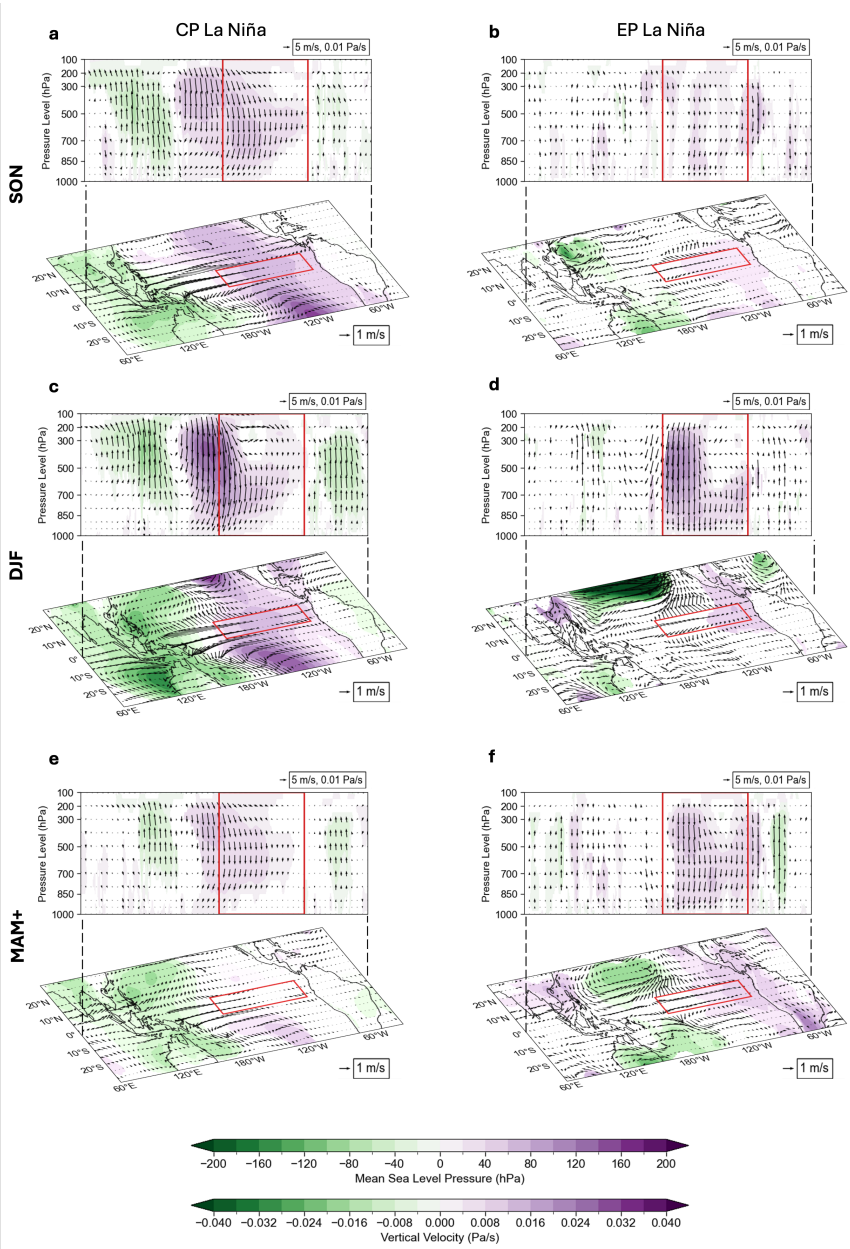

Fig. 5 Seasonal composites of mean sea-level pressure (MSLP), surface wind and vertical velocity anomalies associated with CP and EP La Niña events using 20CRv3 reanalysis (1900-2015). Underlying shading in each plot shows the statistically significant MSLP anomaly; the vectors represent the wind anomalies 100 metres above surface. Shading in the overlaying figure in each subplot shows the statistically significant vertical wind velocity anomaly; the vectors represent the vertical profile of zonal and vertical wind anomalies. For the vectors, the vertical velocities are scaled by a factor of 1000 for visualisation purposes. The vertical wind anomalies and vectors are meridionally averaged between 5°S–5°N. The red box depicts the Niño3.4 region in the tropical Pacific.

season). A low-pressure anomaly in the South Pacific extends westward and includes the Australian continent, which is potentially associated with a strengthening of the descending branches of the Hadley circulation over subtropical Australia and the South Pacific, and the North Pacific which was shown in previous studies [38]. The high-pressure anomalies in the eastern Pacific continue to persist, extending over Central and South America, which is likely associated with the persistence of the descending branch of the Walker Cell (Fig. 5f). Although vertical motion weakens during the decaying stage, these MSLP anomalies persist with strong subtropical highs and mid-latitude lows due to continued ocean–atmosphere coupling via Rossby wave inertia [41]. Our results suggest that this persistence is stronger for EP La Niña events compared to CP La Niña events.

Impacts on precipitation

Strong atmospheric circulation anomalies result in a substantial modulation of large-scale precipitation patterns. Typically, La Niña conditions enhance precipitation over the western Pacific, including the Maritime Continent and northern Australia and the South Pacific Convergence Zone. This is due to increased convection associated with warmer-than-average sea surface temperatures in the western Pacific and a strengthening of the ascending branch of the Pacific Walker Circulation [42, 43]. Conversely, the central and eastern Pacific experience drier-than-normal conditions. The impacts extend beyond the Pacific basin, with La Niña often associated with increased rainfall in the northeastern parts of South America [44, 45], whilst parts of the southern United States [19] and southern South America [46, 47] tend to experience below-average precipitation.

During both types of La Niña events, a distinctive zone with negative rainfall anomalies develops across the tropical Pacific, driven by suppressed convection associated with the cool SST anomalies. For EP La Niña events, this dry zone remains relatively confined to the equatorial Pacific, forming a narrow band of decreased precipitation from the central to eastern Pacific equatorial during developing, mature and decaying phases (Fig. 6b,d,f). By contrast, CP La Niña events are characterised by a markedly different evolution: during the mature phase, the equatorial drying is the most intense compared to other seasons and extends southeastwards into the South Pacific (see Fig. 6c). To the west, northwest and southwest of this region, a positive rainfall anomaly stretches from the Northern Hemisphere through the Western Pacific and towards the southeast, highlighting the intensification of the upward branch of the Pacific Walker Circulation and as well as a strengthening, and potential displacement of the South Pacific Convergence zone [48, 49]. The rainfall increase in this region is absent in the EP La Niña precipitation response, showing opposite sign (dry) rainfall anomalies over much of the region. The mentioned negative rainfall anomalies during CP La Niña events are visible during all event phases. This difference reflects the westward displacement of the strongest negative SST anomalies in CP events, which are substantially stronger than associated with EP events (Fig. 3), which shifts the core of suppressed convection to the west and amplifies the drying signal. During the developing (SON) and decaying (MAM+) stages, both event types show weaker rainfall anomalies than during the mature phase. EP La Niña shows a more zonally

constrained dry band across the equatorial central and eastern Pacific in contrast to CP La Niña events, which show a more pronounced drying footprint in the western Pacific that stretches towards central and South Pacific.

In the off-equatorial region, a stark contrast between EP and CP La Niña events can be observed. During CP La Niña, precipitation is typically enhanced in regions of low-level convergence. As previously indicated, during the developing, mature and decaying phase of CP La Niña events (Fig. 6a,c,e) a significant large-scale increase in precipitation is evident in the off-equatorial diagonal precipitation band in the Southern Hemisphere. This might indicate a south-westward displacement of the SPCZ [49]. In contrast, during EP La Niña events, the approximate region around the SPCZ shows no consistent rainfall anomaly signal (Fig. 6b,d,f). This is a critical event type difference, since this region is home to several small Pacific island nations, which are highly sensitive to the modulation of rainfall patterns on inter-annual timescales [50] that are mainly associated with ENSO events [51, 52].

In addition to broad-scale rainfall anomaly patterns over the mentioned oceanic regions, some key differences also emerge over land. The positive precipitation anomalies over the Maritime Continent and Northern Australia are visible during CP La Niña throughout its life-cycle. Significant wet anomalies during EP La Niña in contrast only occur during the mature phase and are restricted to northern Australia, while parts of the Maritime Continent experience below-average rainfall or insignificant anomalies. Over the Maritime Continent, dry anomalies are apparent during the developing and decay phases, while northern Australia experiences insignificant changes (Fig. 6). Another key difference is seen on the eastern boundary of the Pacific Ocean basin, over the Southern United States. During CP events, dry anomalies occur throughout the La Niña lifecycle, and are strongest during the peak phase. The rainfall response during EP events is inconsistent throughout the seasons. In South America, the strongest rainfall anomalies are visible in the decaying stage of EP events and are characterised by a dipole between a wettening north and drying south of the continent. This stands in contrast to much weaker rainfall anomalies during CP events, likely due to the persistence of vertical wind anomalies and sea level pressure anomalies through boreal spring, as shown previously.

Impacts on biological productivity

Given the key differences in atmospheric and oceanic patterns between EP and CP La Niña events, it is also crucial to look at ocean's biological productivity. Having examined differences in OLR and upwelling patterns based on SST and sub-surface ocean temperatures, we now synthesise these findings to elucidate the collective impact of La Niña event types on ocean biological productivity [53, 54]. This inclusion is crucial, as productivity could significantly differ between either type of La Niña events for marine ecosystems, impacting marine food webs and carbon sequestration capacity [55, 56]. The interplay between light penetration in the upper ocean, fresh-water input due to convection–precipitation changes and upwelling processes can influence the distribution of nutrients that, in turn, creates complex conditions directly influencing the distribution and growth of phytoplankton [57, 58].

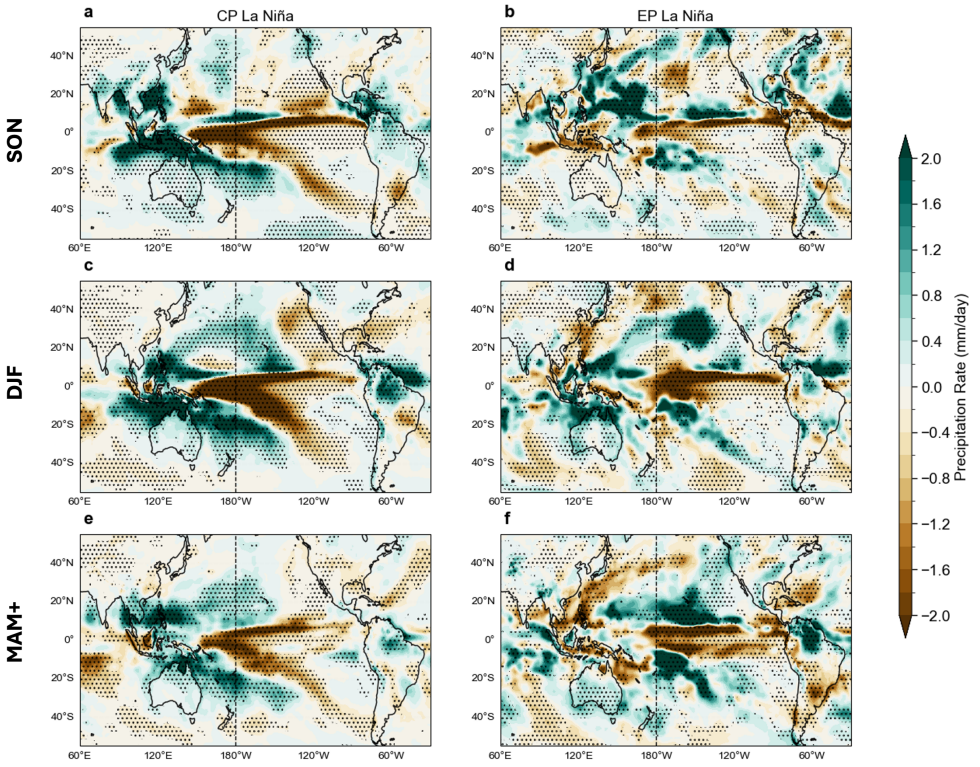

Fig. 6 Seasonal evolution of rainfall anomaly composites associated with CP and EP La Niña events using 20CRv3 (1900-2015). Stippling indicates significance at the 95th percentile. The dashed vertical line represents the 180°W longitude.

Biological productivity variations approximated by Chlorophyll-a concentrations serve as sensitive indicators of ecosystem responses to climate variability [59] and are shown here for the case of CP and EP La Niña events, averaged over the developing through to mature event phase, i.e. from September to February (Fig. 7) to account for the response during the lifecycle of ENSO. We note that the sample size for Chlorophyll-a composites is smaller than for other variables due to limited data availability (1997-2022) with 7 CP La Niña years and 2 EP La Niña years available for the composites. Under climatological conditions, Chlorophyll-a concentrations are higher in the eastern to central equatorial Pacific compared to the western Pacific. (Fig. 7a). This pattern is a result of the eastern equatorial Pacific upwelling and associated cold tongue, leading to nutrient-rich waters that support increased phytoplankton growth. In contrast, the Western Pacific Ward Pool, characterised by warmer, more stratified waters, typically shows lower Chlorophyll-a concentrations, creating a distinct east-west gradient across the basin (Fig. 7a). Equatorial upwelling elevates nutrient levels and Chlorophyll-a concentrations along the equator compared to off-equatorial regions.

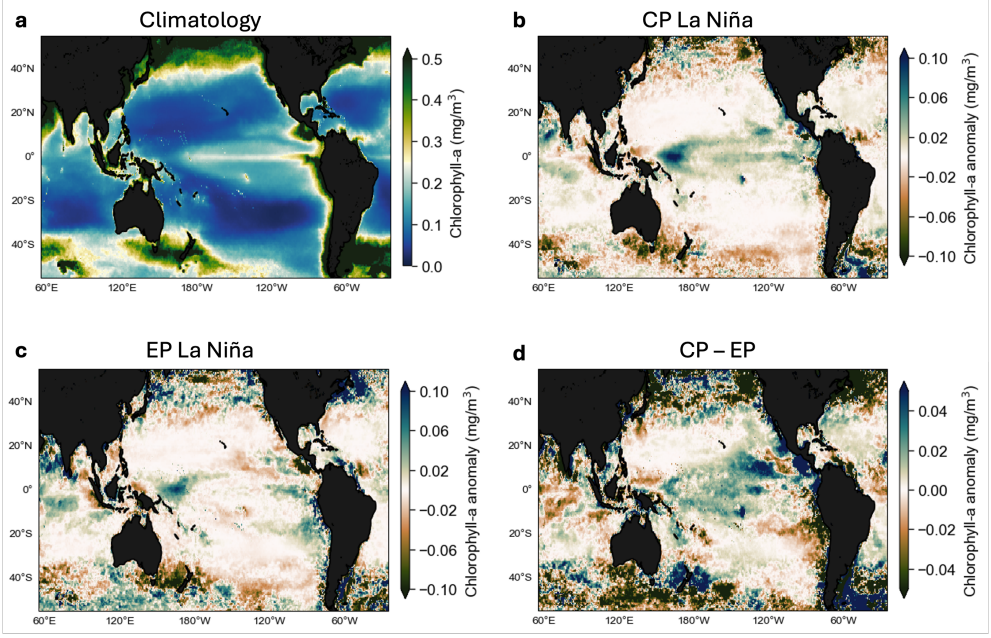

Fig. 7 a) The seasonal climatology (1997-2022) of chlorophyll-a concentrations from September to February alongside the seasonal anomalies during b) CP La Niña years; c) EP La Niña years and d) the difference between CP and EP years.

During CP La Niña events, equatorial upwelling across the entire tropical Pacific is enhanced (Fig. 7b). The most enhanced productivity centre is concentrated in the Western equatorial Pacific. In contrast to the western Pacific, the eastern Pacific upwelling regions show a weaker increase in Chlorophyll-a

During EP La Niña events (Fig. 7c), upwelling off the South American coast, especially around 20°S, is enhanced compared to both the climatology and CP La Niña conditions. This is particularly visible in the difference between CP and EP events (Fig. 7d). The Pacific warm pool region remains a biological active hotspot during both types of La Niña events, but is less pronounced in the EP La Niña composites. Beside the enhance upwelling during EP La Niña events off the South American coast, the productivity across the tropical Pacific basin is less active compared to CP events and shows some areas of weak Chlorophyll-a decreases that flank the equatorial Pacific.

Conclusion

In this paper, we evaluate the oceanic and atmospheric differences between Central Pacific (CP) and Eastern Pacific (EP) La Niña events and their broader climatic implications. CP La Niña events exhibit meridionally broader and more intense sea-surface temperature cooling in the central-to-eastern equatorial Pacific, accompanied by stronger subsurface warming in the western Pacific and a relatively steeper thermocline tilt. EP La Niña events, by contrast, show a more equatorially confined sea surface

temperature cooling pattern restricted to the eastern Pacific, with stronger upwelling anomalies closer to the South American coast and a thermocline response that persists further into the decaying phase of the event (Fig. 8). Atmospheric circulation anomalies are stronger and centred around 180°E during CP events, with the strongest vertical ascent and ocean downwelling in the far western Pacific and a pronounced Pacific Walker circulation strengthening. EP La Niña events are characterised by an eastward shift in atmospheric circulation anomalies and a weaker but more persistent mid-latitude response, including a deepened and equatorward-displaced Aleutian Low during the mature event phase. These contrasting oceanic and atmospheric signatures translate into distinct precipitation and biological productivity anomalies across the Pacific region. CP La Niña events drive broader and more intense drying across the equatorial Pacific during their mature phase. Precipitation is enhanced over the Maritime Continent and Northern Australia throughout the event lifecycle, and persistent dry anomalies are found over the southern United States. EP La Niña events maintain a more equatorially confined dry band, with significant wet anomalies over Northern Australia confined to the mature phase, and the strongest precipitation response in South America occurring during the decaying stage of the event. In terms of biological productivity, CP La Niña events show enhanced equatorial upwelling across the broad tropical Pacific region, with productivity increases particularly concentrated in the western Pacific warm pool region. In contrast, EP La Niña events drive stronger upwelling off the South American coast but show reduced productivity across much of the tropical Pacific basin (Fig. 7d).

Even though La Niña diversity has received less attention compared to EL Niño diversity, it carries meaningful consequences for regional climate assessment. Regions such as South America, the Maritime Continent, Pacific island nations, and parts of Asia would benefit from a more differentiated view of La Niña events when interpreting teleconnection patterns and associated hydrological impacts. Subtle zonal differences in SST cooling location can drive differences in convective organisation and Walker circulation strength and location, leading to cascading effects on precipitation, freshwater input, mixed layer dynamics, thermocline depth, and ultimately marine biological productivity. The distinctions between different types of La Niña events matter not only for understanding land-based agricultural and societal risks, but also for quantifying ecosystem responses in the ocean.

Our study represents a conservative characterisation of CP and EP La Niña differences due to a relatively small number of clearly classifiable observed events, especially EP events ($n = 5$). We deliberately chose to include only those events identified across multiple long observational datasets to increase our confidence in the composite results, while compromising on sample size (see Data section). CP and EP La Niña events remain less distinct from each other compared to their El Niño counterparts [60], and a substantial proportion of La Niña events fall into a mixed category that resists clean classification (see Table A1). Future work could extend this framework to better characterise these ambiguous events, and to examine whether the distinctions documented here are faithfully captured in coupled climate models [61]; a necessary step for building confidence in projected changes to diverse La Niña characteristics.

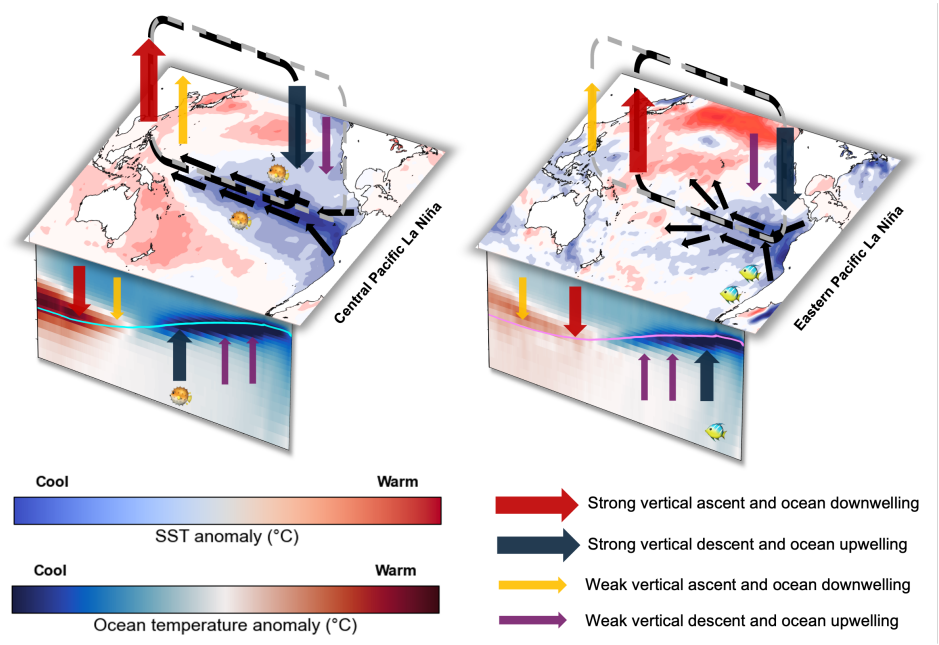

Fig. 8 Schematic of the atmospheric and oceanic response during CP and EP La Niña events. During CP events, strong equatorial easterly winds are prevalent alongside a stronger zonal Pacific Walker circulation response, with deeper and westward shifted vertical ascent in the Western Pacific accompanied by descent in the Eastern Pacific. The ocean subsurface warming in the Western Pacific and cooling in the Eastern Pacific are also more prominent, with a steeper thermocline response to surface winds. As a result, there are stronger downwelling anomalies in the Western Pacific and upwelling anomalies in the Eastern Pacific. In contrast, during EP events, a relatively weaker easterly wind response coincides with a weaker and eastward shifted Walker circulation compared to CP events. Alongside the weaker atmospheric response, the subsurface temperature anomalies are much warmer in the Central Pacific and cooler near the continental margins, indicative of a deeper thermocline in the central Pacific and relatively shallower thermocline near the continental margins.

Distinguishing between different types of La Niña events is particularly relevant given climate model projections suggesting an increased frequency of consecutive and prolonged La Niña events under continued greenhouse warming [9–11]. Should multi-year La Niña sequences become more common, the diversity of La Niña types and the potential for alternating CP and EP events within a single multi-year episode, as observed during 2020–23 will need to be explicitly accounted for in assessments of regional hydroclimatic risk, drought development, and hydrological disruption. The framework presented here provides a foundation for that task.

Data

Our study analyses different observational, model, and reanalysis data post 1900. Sea surface temperatures (SSTs) from the following three observational products

between 1900 and 2023 were used: the Hadley Centre Global Sea Ice and Sea Surface Temperature version 1.1 (HadISST v1.1) dataset [62], the extended reconstructed sea-surface temperature reanalysis (ERSST) version 5 [63] and the Centennial in-situ Observation-based Estimates (COBE) SST analysis dataset version 2 [64]. Atmospheric variables were obtained from the 20th century reanalysis version 3 (20CRv3): OLR, mean sea level pressure (MSLP), low level (100 metres) horizontal winds, vertical winds, as well as horizontal winds at different levels, surface air temperature and precipitation rate for the time period 1900 to 2015 [34]. Chlorophyll-a is obtained from European Space Agency Ocean Colour Climate Change Initiative project (ESA OC-CCI) version 6.0 for the period 1997-2022 [65]. The subsurface temperatures in the equatorial Pacific are derived from a global ocean–sea ice model simulation of ACCESS-OM2 [66] at 0.10° lateral resolution forced with the JRA55-do atmospheric reanalysis [67] spanning 1958–2023.

Methods

ENSO classification

We first identify different types of La Niña by performing Empirical Orthogonal Function (EOF) analysis on observed, seasonally averaged tropical Pacific SSTs (15°S–15°N, 140°E–80°W) similar to [26, 68]. Prior to the EOF analysis, the seasonal climatology based on the full length of the SST record is removed and the SST record is quadratically detrended. The resulting first and second principal components are used. A La Niña event is defined when the first principal component (PC1) falls below -0.5 standard deviations for at least two consecutive seasons. Events are then partitioned by the sign of the second principal component (PC2): an event is classified as a Central Pacific (CP) La Niña when PC2 ≤ 0 and as an Eastern Pacific (EP) La Niña when PC2 ≥ 0. The analysis is applied to HadISST, ERSST, and COBE SSTs to objectively classify Central and Eastern Pacific La Niña events that consistently occur across multiple datasets. An event is included here as a CP or EP La Niña when at least two out of these three datasets agree on the occurrence of the respective type of La Niña event and its classification. A list of all resulting La Niña event years is included in Table A1. The listed year refers to the start year of the event. For the ACCESS-OM2-01, we perform the same analysis on the model output SSTs. To ensure consistency with the other products, we only consider those CP and EP La Niña events in the ACCESS-OM2-01 that have been obtained from the analysis above (see Table A1).

La Niña events primarily occur in the central Pacific, with a considerably lower number of events originating in the eastern Pacific. The distinction between CP and EP La Niña events is far less distinctive and less independent compared to their El Niño counterparts [22].

The analysis is based on composites resulting from all CP and EP La Niña events following our classification. Given the limited number of observed events, significance is assessed by bootstrapping all composites. This involved resampling with replacement 1000 times and identifying regions where at least 95% of the bootstrapped samples agreed on the sign of the anomaly.

Acknowledgements. This research uses the ACCESS-NRI's ACCESS-OM2-01 model infrastructure, which is enabled by the Australian Government's National Collaborative Research Infrastructure Strategy (NCRIS). Furthermore, our research was undertaken with the assistance of computational resources from the National Computational Infrastructure, an NCRIS-enabled capability supported by the Australian Government. We would like to thank the vibrant community of the Consortium for Ocean–Sea Ice Modelling in Australia (COSIMA; cosima.org.au) for fruitful discussions, for maintaining the collection of the COSIMA Cookbook notebooks [69], and for making the output of the ACCESS-OM2-01 model publicly available.

Funding sources. We acknowledge funding from the National Environmental Science Program Climate systems Hub (H.H.) and from the Australian Research Council under the Center of Excellence for the Weather of the 21st Century CE230100012 (M.B.F., A.S., and N.C.C.) and the Discovery Project DP240101274 (N.C.C.).

Conflict of interest. The authors declare no conflict of interest.

Data availability. The Hadley Centre Global Sea Ice and Sea Surface Temperature version 1.1 (HadISST v1.1) dataset [62] is available at www.metoffice.gov.uk/hadobs/hadisst. The extended reconstructed sea-surface temperature reanalysis version 5 (ERSSTv5) [63] is available at doi:10.7289/V5T72FNM. The Centennial in-situ Observation-based Estimates (COBE) SST analysis dataset version 2 [64] is available at www.esrl.noaa.gov/psd/data/gridded/data.cobe2.html. NOAA/CIRES/DOE 20th Century Reanalysis (V3) data as described in [34] is provided by NOAA PSL, Boulder, Colorado, USA, from their website at . The European Space Agency Ocean Colour Climate Change Initiative project (ESA OC-CCI) version 6.0 [65] is available at www.oceancolour.org. The ACCESS-OM2-01 ocean–sea ice model output is available at doi: 10.4225/41/5a2dc8543105a

Code availability. Scripts and Jupyter notebooks for reproducing the analyses and figures are available at the GitHub repository github.com/navidcy/LaNina-flavours.

Author Contribution. The study was initially conceived by M.B.F. and H.H., who also carried out the preliminary analysis. The project was then expanded on and refined by all the authors team, who contributed to the development of the final analyses, preparation of figures, and discussion of results. All authors participated in several day-long hackathons in 2025 that significantly helped to push this project forward. M.B.F. drafted an early version of the manuscript; H.H., A.S., R.L., and N.C.C. reviewed and revised the draft.

Appendix A Classification of La Niña events

In this appendix, we provide a list of La Niña events from 1900-2023, referring to the start year of the event. The event classification is conducted using the method by Chen et al. [68]. Events are defined as CP or EP La Niñas, when the classification identifies a CP or EP event respectively in at least two out of three observational SST datasets: HadISST, ERSST, and COBE. Events are defined as 'Mixed' when the

Table A1 List of La Niña events from 1900-2023 and their classification (Central Pacific (CP); Eastern Pacific (EP); Mixed).

CP La Nina	EP La Nina	Mixed La Nina
1903	1906	1908
1909	1962	1910
1924	1967	1916
1933	2017	1917
1938	2021	1922
1942		1949
1950		1995
1954		
1955		
1964		
1970		
1971		
1973		
1974		
1975		
1984		
1988		
1998		
1999		
2000		
2007		
2010		
2011		
2020		
2022		

classification across datasets does not agree on whether a CP or EP type event took place. The results for 'Mixed' events are excluded for the remainder of this analysis.

References

[1] McPhaden, M.J., Zebiak, S.E., Glantz, M.H.: ENSO as an integrating concept in Earth science. Science **314**(5806), 1740–1745 (2006) https://doi.org/10.1126/science.1132588

[2] Callahan, C.W., Mankin, J.S.: Persistent effect of El Niño on global economic growth. Science **380**(6649), 1064–1069 (2023) https://doi.org/10.1126/science.adf2983

[3] Anderson, W., Seager, R., Baethgen, W., Cane, M., You, L.: Synchronous crop failures and climate-forced production variability. Science Advances **5**(7), 1976 (2019) https://doi.org/10.1126/sciadv.aaw1976

[4] Capotondi, A., Wittenberg, A.T., Newman, M., Lorenzo, E.D., Yu, J.-Y., Braconnot, P., Cole, J., Dewitte, B., Giese, B., Guilyardi, E., Jin, F.-F., Karnauskas, K., Kirtman, B., Lee, T., Schneider, N., Xue, Y., Yeh, S.-W.: Understanding ENSO Diversity. Bulletin of the American Meteorological Society **96**(6), 921–938 (2015) https://doi.org/10.1175/BAMS-D-13-00117.1

[5] Timmermann, A., An, S.-I., Kug, J.-S., Jin, F.-F., Cai, W., Capotondi, A., Cobb, K.M., Lengaigne, M., McPhaden, M.J., Stuecker, M.F., *et al.*: El niño–southern oscillation complexity. Nature **559**(7715), 535–545 (2018) https://doi.org/10.1038/s41586-018-0252-6

[6] Okumura, Y.M.: ENSO diversity from an atmospheric perspective. Current Climate Change Reports **5**(3), 245–257 (2019) https://doi.org/10.1007/s40641-019-00138-7

[7] Capotondi, A., Wittenberg, A.T., Kug, J.-S., Takahashi, K., McPhaden, M.J.: 4. ENSO Diversity, pp. 65–86. American Geophysical Union (AGU), ??? (2020). https://doi.org/10.1002/9781119548164.ch4

[8] Liu, Y., Tao, W., Huang, G., Wang, Y., Hu, K., Liu, Y.: Contrasting impact of single-year and multi-year El Niño on the Pacific-North American teleconnection pattern. Environmental Research Letters **19**(12), 124056 (2024) https://doi.org/10.1088/1748-9326/ad9038

[9] Cai, W., Wang, G., Santoso, A., McPhaden, M.J., Wu, L., Jin, F.-F., Timmermann, A., Collins, M., Vecchi, G., Lengaigne, M., England, M.H., Dommenget, D., Takahashi, K., Guilyardi, E.: Increased frequency of extreme La Niña events under greenhouse warming. Nature Climate Change **5**(2), 132–137 (2015) https://doi.org/10.1038/nclimate2492

[10] Wang, B., Sun, W., Jin, C., Luo, X., Yang, Y.-M., Li, T., Xiang, B., McPhaden, M.J., Cane, M.A., Jin, F., Liu, F., Liu, J.: Understanding the recent increase in multiyear La Niñas. Nature Climate Change **13**(10), 1075–1081 (2023) https:

//doi.org/10.1038/s41558-023-01801-6

[11] Geng, T., Jia, F., Cai, W., Wu, L., Gan, B., Jing, Z., Li, S., McPhaden, M.J.: Increased occurrences of consecutive La Niña events under global warming. Nature **619**(7971), 774–781 (2023) https://doi.org/10.1038/s41586-023-06236-9

[12] Rasmusson, E.M., Carpenter, T.H.: Variation in tropical sea surface temperature and surface wind fields associated with the Southern Oscillation/El Niño. Monthly Weather Review **110**, 354 (1982) https://doi.org/10.1175/1520-0493(1982)110⟨0354:VITSST⟩2.0.CO;2

[13] Reid, K.J., Barnes, M.A., Gillett, Z.E., Parker, T., Udy, D.G., Ayat, H., Boschat, G., Bowden, A., Grosfeld, N.H., King, A.D.: A multiscale evaluation of the wet 2022 in Eastern Australia. Journal of Climate **38**(4), 909–929 (2025) https://doi.org/10.1175/JCLI-D-24-0224.1

[14] Hernández Ayala, J.J., Méndez-Tejeda, R.: The extremely active 2020 hurricane season in the North Atlantic and its relation to climate variability and change. Atmosphere **13**(12), 1945 (2022) https://doi.org/10.3390/atmos13121945

[15] Anderson, W., Cook, B.I., Slinski, K., Schwarzwald, K., McNally, A., Funk, C.: Multiyear La Niña events and multiseason drought in the Horn of Africa. Journal of Hydrometeorology **24**(1), 119–131 (2023) https://doi.org/10.1175/jhm-d-22-0043.1

[16] Zhang, T., Zhang, W., Jiang, F., Hu, S., Sun, S., Jin, F.-F., Chen, H.: Pan-regional prolonged droughts linked to consecutive La Niña events. Geophysical Research Letters **53**(12), 2026–122176 (2026) https://doi.org/10.1029/2026GL122176

[17] Jones, N.: Rare 'triple' La Niña climate event looks likely — what does the future hold? Nature **607**(7917), 21–21 (2022) https://doi.org/10.1038/d41586-022-01668-1

[18] Cole, J.E., Overpeck, J.T., Cook, E.R.: Multiyear La Niña events and persistent drought in the contiguous United States. Geophysical Research Letters **29**(13), 25–1254 (2002) https://doi.org/10.1029/2001GL013561

[19] Okumura, Y.M., DiNezio, P., Deser, C.: Evolving impacts of multiyear La Niña events on atmospheric circulation and U.S. drought. Geophysical Research Letters **44**(22), 11614–11623 (2017) https://doi.org/10.1002/2017gl075034

[20] Deepak, S.N.R., Chowdary, J.S., Dandi, A.R., Srinivas, G., Parekh, A., Gnanaseelan, C., Yadav, R.K.: Impact of multiyear La Niña events on the South and East Asian summer monsoon rainfall in observations and CMIP5 models. Climate Dynamics **52**(11), 6989–7011 (2019) https://doi.org/10.1007/s00382-018-4561-0

[21] Ashok, K., Behera, S.K., Rao, S.A., Weng, H., Yamagata, T.: El Niño Modoki and

its possible teleconnection. Journal of Geophysical Research: Oceans **112**(C11), 11007 (2007) https://doi.org/10.1029/2006JC003798

[22] Kug, J., Ham, Y.: Are there two types of La Niña? Geophysical Research Letters **38**(16), 16704 (2011) https://doi.org/10.1029/2011GL048237

[23] Sun, L., Taschetto, A.S., McGregor, S., Alexander, L.V.: Diverse impacts of Eastern Pacific and central Pacific ENSO on Australian spring rainfall and associated Southern hemisphere large-scale circulation. Journal of Climate, 250606 (2026) https://doi.org/10.1175/JCLI-D-25-0606.1

[24] Iskandar, I., Lestari, D.O., Masumoto, Y.: La Niña Modoki enhanced summer-autumn precipitation over the Indonesian region. Asia-Pacific Journal of Atmospheric Sciences **58**(4), 507–517 (2022) https://doi.org/10.1007/s13143-022-00271-8

[25] Wei, Y., Ren, H.: Distinct MJOs under the two types of La Niña. Journal of Geophysical Research: Atmospheres **127**(23), 2022–037646 (2022) https://doi.org/10.1029/2022JD037646

[26] Freund, M.B., Brown, J.R., Marshall, A.G., Tozer, C.R., Henley, B.J., Risbey, J.S., Ramesh, N., Lieber, R., Sharmila, S.: Interannual ENSO diversity, transitions, and projected changes in observations and climate models. Environmental Research Letters **19**(11), 114005 (2024) https://doi.org/10.1088/1748-9326/ad78db

[27] Wang, G., Santoso, A.: Multi-year La Niña frequency tied to southward tropical Pacific wind shift. npj Climate and Atmospheric Science **7**(1), 226 (2024) https://doi.org/10.1038/s41612-024-00772-5

[28] Lu, Z., Schultze, A., Carré, M., Brierley, C., Hopcroft, P.O., Zhao, D., Zheng, M., Braconnot, P., Yin, Q., Jungclaus, J.H., Shi, X., Yang, H., Zhang, Q.: Increased frequency of multi-year El Niño–Southern Oscillation events across the Holocene. Nature Geoscience **18**(4), 337–343 (2025) https://doi.org/10.1038/s41561-025-01670-y

[29] Wu, X., Okumura, Y.M., DiNezio, P.N.: What controls the duration of El Niño and La Niña events? Journal of Climate **32**(18), 5941–5965 (2019) https://doi.org/10.1175/JCLI-D-18-0681.1

[30] Hasan, N.A., Chikamoto, Y., McPhaden, M.J.: The influence of tropical basin interactions on the 2020–2022 double-dip La Niña. Frontiers in Climate **4**, 1001174 (2022) https://doi.org/10.3389/fclim.2022.1001174

[31] Kim, J.-W., Yu, J.-Y., Tian, B.: Overemphasized role of preceding strong El Niño in generating multi-year La Niña events. Nature Communications **14**(1), 6790 (2023) https://doi.org/10.1038/s41467-023-42373-5

[32] Iwakiri, T., Watanabe, M.: Mechanisms linking multi-year La Niña with preceding strong El Niño. Scientific Reports **11**(1), 17465 (2021) https://doi.org/10.1038/s41598-021-96056-6

[33] Freund, M.B., Henley, B.J., Karoly, D.J., McGregor, H.V., Abram, N.J., Dommenget, D.: Higher frequency of Central Pacific El Niño events in recent decades relative to past centuries. Nature Geoscience **6**, 450–455 (2019) https://doi.org/10.1038/s41561-019-0353-3

[34] Slivinski, L.C., Compo, G.P., Whitaker, J.S., Sardeshmukh, P.D., Giese, B.S., McColl, C., Allan, R., Yin, X., Vose, R., Titchner, H., Kennedy, J., Spencer, L.J., Ashcroft, L., Brönnimann, S., Brunet, M., Camuffo, D., Cornes, R., Cram, T.A., Crouthamel, R., Domínguez-Castro, F., Freeman, J.E., Gergis, J., Hawkins, E., Jones, P.D., Jourdain, S., Kaplan, A., Kubota, H., Blancq, F.L., Lee, T., Lorrey, A., Luterbacher, J., Maugeri, M., Mock, C.J., Moore, G.W.K., Przybylak, R., Pudmenzky, C., Reason, C., Slonosky, V.C., Smith, C.A., Tinz, B., Trewin, B., Valente, M.A., Wang, X.L., Wilkinson, C., Wood, K., Wyszyński, P.: Towards a more reliable historical reanalysis: Improvements for version 3 of the twentieth century reanalysis system. Quarterly Journal of the Royal Meteorological Society **145**, 2876–2908 (2019) https://doi.org/10.1002/qj.3598

[35] Wyrtki, K.: El Niño—The dynamic response of the equatorial Pacific ocean to atmospheric forcing. Journal of Physical Oceanography **5**(4), 572–584 (1975) https://doi.org/10.1175/1520-0485(1975)005⟨0572:entdro⟩2.0.co;2

[36] Holton, J.R., Curry, J.A., Pyle, J.A. (eds.): Encyclopedia of Atmospheric Sciences. Academic Press, Amsterdam (2002)

[37] Wills, R.C., Dong, Y., Proistosecu, C., Armour, K.C., Battisti, D.S.: Systematic climate model biases in the large-scale patterns of recent sea-surface temperature and sea-level pressure change. Geophysical Research Letters **49**(17), 2022–100011 (2022) https://doi.org/10.1029/2022GL100011

[38] Guo, Y.-P., Li, J.-P.: Impact of ENSO events on the interannual variability of Hadley circulation extents in boreal winter. Advances in Climate Change Research **7**(1-2), 46–53 (2016) https://doi.org/10.1016/j.accre.2016.05.001

[39] Trenberth, K.E., Paolino, D.A.: Characteristic patterns of variability of sea level pressure in the Northern Hemisphere. Monthly Weather Review **109**(6), 1169–1189 (1981) https://doi.org/10.1175/1520-0493(1981)109⟨1169:CPOVOS⟩2.0.CO;2

[40] Wallace, J.M., Gutzler, D.S.: Teleconnections in the geopotential height field during the Northern Hemisphere winter. Monthly weather review **109**(4), 784–812 (1981) https://doi.org/10.1175/1520-0493(1981)109⟨0784:TITGHF⟩2.0.CO;2

[41] Wirth, V., Riemer, M., Chang, E.K.M., Martius, O.: Rossby Wave packets on the

midlatitude waveguide — A review. Monthly Weather Review **146**(7), 1965–2001 (2018) https://doi.org/10.1175/mwr-d-16-0483.1

[42] Taschetto, A.S., Ummenhofer, C.C., Stuecker, M.F., Dommenget, D., Ashok, K., Rodrigues, R.R., Yeh, S.-W.: ENSO Atmospheric Teleconnections, pp. 309–335. American Geophysical Union (AGU), ??? (2020). Chap. 14. https://doi.org/10.1002/9781119548164.ch14

[43] Lieber, R., Brown, J., King, A., Freund, M.: Historical and future asymmetry of enso teleconnections with extremes. Journal of Climate **37**(22), 5909–5924 (2024) https://doi.org/10.1175/JCLI-D-23-0619.1

[44] Grimm, A.M.: Interannual climate variability in South America: impacts on seasonal precipitation, extreme events, and possible effects of climate change. Stochastic Environmental Research and Risk Assessment **25**(4), 537–554 (2011) https://doi.org/10.1007/s00477-010-0420-1

[45] Lopes, A.B., Andreoli, R.V., Souza, R.A., Cerón, W.L., Kayano, M.T., Canchala, T., Moraes, D.S.: Multiyear La Niña effects on the precipitation in South America. International Journal of Climatology **42**(16), 9567–9582 (2022) https://doi.org/10.1002/joc.7847s

[46] Grimm, A.M., Barros, V.R., Doyle, M.E.: Climate variability in southern South America associated with El Niño and La Niña events. Journal of climate **13**(1), 35–58 (2000) https://doi.org/10.1175/1520-0442(2000)013⟨0035:CVISSA⟩2.0.CO;2

[47] Grimm, A.M., Tedeschi, R.G.: ENSO and extreme rainfall events in South America. Journal of Climate **22**(7), 1589–1609 (2009) https://doi.org/10.1175/2008JCLI2429.1

[48] Narsey, S., Brown, J.R., Delage, F., Boschat, G., Grose, M., Colman, R., Power, S.: Storylines of South Pacific convergence zone changes in a warmer world. Journal of Climate **35**(20), 6549–6567 (2022) https://doi.org/10.1175/JCLI-D-21-0433.1

[49] Brown, J.R., Lengaigne, M., Lintner, B.R., Widlansky, M.J., Der Wiel, K., Dutheil, C., Linsley, B.K., Matthews, A.J., Renwick, J.: South Pacific convergence zone dynamics, variability and impacts in a changing climate. Nature Reviews Earth & Environment **1**(10), 530–543 (2020) https://doi.org/10.1038/s43017-020-0078-2

[50] Mycoo, M., Wairiu, M., Campbell, D., Duvat, V., Golbuu, Y., Maharaj, S., Nalau, J., Nunn, P., Pinnegar, J., Warrick, O., Anderson, G., Cruz, F., Devenish-Nelson, E., Ebi, K., Loehr, J., Mahon, R., McNaught, R., Parsons, M., Price, J., Robinson, S.-A., Thomas, A.: In: Pörtner, H.-O., Roberts, D., Tignor, M., Poloczanska, E., Mintenbeck, K., Alegría, A., Craig, M., Langsdorf, S., Löschke, S., Möller, V.,

Okem, A., Rama, B. (eds.) Small Islands. Cambridge University Press, United States (2022). https://doi.org/10.1017/9781009325844.017

[51] Pagli, B., Izumo, T., Cravatte, S., Hopuare, M., Martinoni-Lapierre, S., Laurent, V., Menkès, C., Monselesan, D., Auffray, S.: The diverse impacts of El Niño and La Niña events over the South Pacific and in French Polynesia. Journal of Climate **38**(12), 2681–2701 (2025) https://doi.org/10.1175/JCLI-D-24-0408.1

[52] Salinger, M.J., Lefale, P.: In: Sivakumar, M.V.K., Motha, R.P., Das, H.P. (eds.) The occurrence and predictability of extreme events over the Southwest Pacific with particular reference to ENSO, pp. 39–49. Springer, Berlin, Heidelberg (2005). https://doi.org/10.1007/3-540-28307-2_3

[53] Chen, R., Wu, B., Li, Z., Wang, S.: Impacts of ENSO on tropical pacific chlorophyll biomass under historical and RCP8.5 scenarios. Journal of Geophysical Research: Oceans **129**(4) (2024) https://doi.org/10.1029/2023jc020720

[54] An, L., Laws, E.A., Liu, X., Chen, R., Wang, S., Hu, S., Zhang, Y., Huang, Y., Xu, F., Chai, F., Huang, B.: Contrasting climate oscillations impacts on phytoplankton in the western and eastern tropical Pacific. Nature Communications **16**(1), 10931 (2025) https://doi.org/10.1038/s41467-025-65947-x

[55] Lin, L., Xu, K., Tan, W., Liu, J., Chen, B., Liu, D.: Amplifying effects of multiyear La Niña on phytoplankton biomass in the tropical Pacific. Limnology and Oceanography Letters **11**(3), 70143 (2026) https://doi.org/10.1002/lol2.70143

[56] Pennington, J.T., Mahoney, K.L., Kuwahara, V.S., Kolber, D.D., Calienes, R., Chavez, F.P.: Primary production in the eastern tropical Pacific: A review. Progress in oceanography **69**(2-4), 285–317 (2006) https://doi.org/10.1016/j.pocean.2006.03.012

[57] An, L., Laws, E.A., Liu, X., Chen, R., Wang, S., Hu, S., Zhang, Y., Huang, Y., Xu, F., Chai, F., *et al.*: Contrasting climate oscillations impacts on phytoplankton in the western and eastern tropical Pacific. Nature Communications **16**(1), 10931 (2025) https://doi.org/10.1038/s41467-025-65947-x

[58] Chen, R., Wu, B., Li, Z., Wang, S.: Impacts of ENSO on tropical Pacific chlorophyll biomass under historical and RCP8.5 scenarios. Journal of Geophysical Research: Oceans **129**(4), 2023–020720 (2024) https://doi.org/10.1029/2023JC020720

[59] Huot, Y., Babin, M., Bruyant, F., Grob, C., Twardowski, M., Claustre, H.: Does chlorophyll a provide the best index of phytoplankton biomass for primary productivity studies? Biogeosciences Discussions **4**(2), 707–745 (2007) https://doi.org/10.5194/bgd-4-707-2007

[60] Kug, J.-S., Jin, F.-F., An, S.-I.: Two types of El Niño Events: Cold tongue El

Niño and warm pool El Niño. Journal of Climate **22**(6), 1499–1515 (2009) https://doi.org/10.1175/2008JCLI2624.1

[61] Taschetto, A.S., Gupta, A.S., Jourdain, N.C., Santoso, A., Ummenhofer, C.C., England, M.H.: Cold tongue and warm pool ENSO events in CMIP5: Mean state and future projections. Journal of Climate **27**(8), 2861–2885 (2014) https://doi.org/10.1175/jcli-d-13-00437.1

[62] Rayner, N.A., Parker, D.E., Horton, E.B.: Global analyses of sea surface temperature, sea ice, and night marine air temperature since the late nineteenth century. Journal of Geophysical Research: Atmospheres **108**(D14), 4407 (2003) https://doi.org/10.1029/2002JD002670

[63] Huang, B., Thorne, P.W., Banzon, V.F., Boyer, T., Chepurin, G., Lawrimore, J.H., Menne, M.J., Smith, T.M., Vose, R.S., Zhang, H.-M.: Extended Reconstructed Sea Surface Temperature, Version 5 (ERSSTv5): Upgrades, validations, and intercomparisons. Journal of Climate **30**(20), 8179–8205 (2017) https://doi.org/10.1175/JCLI-D-16-0836.1

[64] Hirahara, S., Ishii, M., Climate, Y.F.J.o., 2014: Centennial-scale sea surface temperature analysis and its uncertainty. Journal of Climate (2014) https://doi.org/10.1175/JCLI-D-12-00837.1

[65] Sathyendranath, S., Jackson, T., Brockmann, C., Brotas, V., Calton, B., Chuprin, A., Clements, O., Cipollini, P., Danne, O., Dingle, J., Donlon, C., Grant, M., Groom, S., Krasemann, H., Lavender, S., Mazeran, C., Mélin, F., Müller, D., Steinmetz, F., Valente, A., Zühlke, M., Feldman, G., Franz, B., Frouin, R., Werdell, J., Platt, T.: ESA Ocean Colour Climate Change Initiative (Ocean_Colour_cci): Version 6.0, 4km resolution data. NERC EDS Centre for Environmental Data Analysis (2023). https://doi.org/10.5285/5011D22AAE5A4671B0CBC7D05C56C4F0 . https://catalogue.ceda.ac.uk/uuid/5011d22aae5a4671b0cbc7d05c56c4f0

[66] Kiss, A.E., Hogg, A.M., Hannah, N., Dias, F.B., Brassington, G.B., Chamberlain, M.A., Chapman, C., Dobrohotoff, P., Domingues, C.M., Duran, E.R., England, M.H., Fiedler, R., Griffies, S.M., Heerdegen, A., Heil, P., Holmes, R.M., Klocker, A., Marsland, S.J., Morrison, A.K., Munroe, J., Nikurashin, M., Oke, P.R., Pilo, G.S., Richet, O., Savita, A., Spence, P., Stewart, K.D., Ward, M.L., Wu, F., Zhang, X.: ACCESS-OM2 v1.0: A global ocean-sea ice model at three resolutions. Geoscientific Model Development **13**, 401–442 (2020) https://doi.org/10.5194/gmd-13-401-2020

[67] Tsujino, H., Urakawa, S., Nakano, H., Small, R.J., Kim, W.M., Yeager, S.G., Danabasoglu, G., Suzuki, T., Bamber, J.L., Bentsen, M., Böning, C.W., Bozec, A., Chassignet, E.P., Curchitser, E., Dias, F.B., Durack, P.J., Griffies, S.M., Harada, Y., Ilicak, M., Josey, S.A., Kobayashi, C., Kobayashi, S., Komuro, Y., Large, W.G., Sommer, J.L., Marsland, S.J., Masina, S., Scheinert, M., Tomita,

H., Valdivieso, M., Yamazaki, D.: JRA55 based surface dataset for driving ocean–sea-ice models (JRA55-do). Ocean Modelling **130**, 79–139 (2018) https://doi.org/10.1016/j.ocemod.2018.07.002

[68] Chen, C., Cane, M.A., Wittenberg, A.T., Chen, D.: ENSO in the CMIP5 Simulations: Life cycles, diversity, and responses to climate change. Journal of Climate **30**(2), 775–801 (2017) https://doi.org/10.1175/JCLI-D-15-0901.1

[69] Constantinou, N.C., Hogg, A.M., Gibson, A., Steketee, A., Beucher, R., Proft, M., Heerdegen, A., Neme, J., Holmes, R.M., Morrison, A., Fierro-Arcos, D., Kiss, A.E., Oliveira, M., Yung, C., Doddridge, E., Huneke, W., Bhagtani, D., Ong, E.Q.Y., Munroe, J., Schmidt, C., Dawson, H., Squire, D.T., Dias, F.B., Jeffree, J., Moorman, R., Martínez-Moreno, J., Zika, J., Meijer, J.J., Auger, M., Aguiar, W., Moore, T., Silva, F., Yang, L., White, M., Sohail, T., Barnes, A.J., Spence, P., Turner, C., Rosevear, M.G., Bull, C.Y.S., Day, N., Li, M., Ellepola, A., Narayanan, A.: COSIMA Cookbook: A cookbook of recipes for analysing ocean and sea ice model output. Zenodo (2026) https://doi.org/10.5281/zenodo.18283609